Short Communication

Facile Synthesis and Electrochemical Study of CuO Thin Films for Hydrogen Peroxide Reduction in Alkaline Medium

Abderrazak Hamam[1,], Charif Dehchar[1], Mounira Maiza[1], Imene Chikouche[2], Halim Merabti[1]*

[1] Research Center in Industrial Technologies CRTI, P.O. Box 64, Cheraga 16014, Algiers, Algeria
[2] Laboratoire Croissance et Caractérisation de Nouveaux Semi-conducteurs, Université Ferhat Abbas, Sétif-1, Algérie
[*]E-mail: hamam.abderrazak@yahoo.com

In this work, we describe a simple electrochemical procedure for synthesis of structured copper (II) oxide (CuO) films on copper (Cu) substrate for the reduction of hydrogen peroxide (H_2O_2). Films are grown in a single step by direct electrochemical oxidation of Cu foil from a solution of 5 M KOH using cyclic voltammetry method. Scanning electron microscopy images reveal that CuO is uniformly grown on the surface of the substrate and presents a lawn-like microstructure. Electrocatalytic activity of the electrode toward hydrogen peroxide reduction is investigated by cyclic voltammetry and chronoamperometry in 3.0 M KOH solution. The prepared electrode exhibits remarkable catalytic activity, good reproducibility and stable electrochemical response.

1. INTRODUCTION

Hydrogen peroxide (H_2O_2) is an important chemical species in various fields such as environmental science, clinical diagnostics, food processes, chemical industries and biochemistry [1, 2]. Recently, H_2O_2 has been recognized as an alternative oxidizer in fuel cells instead of oxygen, particularly, for several types of low temperature liquid-based fuel cells, including direct hydrazine/hydrogen peroxide fuel cell [3], direct borohydride/hydrogen peroxide fuel cell [4], direct formic acid/hydrogen peroxide fuel cell [5] and biofuel/hydrogen peroxide fuel cell [6]. In comparison with oxygen, H_2O_2 has many advantages: (i) H_2O_2 has high electrochemical reactivity [7]. (ii) Its electroreduction is kinetically faster than O_2 electroreduction since it has a much lower activation barrier, and, moreover, it takes place via a two-electron transfer process and therefore more efficient [8, 9]. (iii) H_2O_2 is used in liquid phase and thus handled and stored more easily. (iv) The electromotive force (EMF)

of the fuel cell using H_2O_2 as the oxidizer was experimentally proved to be much higher than that using O_2 as the oxidizer [10]. (v) Finally, the fuel cell using H_2O_2 is more compact in size [11].

In recent years, in order to efficiently achieve H_2O_2 reduction, intensive research effort has been put into the design of novel electrocatalysts. The available literature suggests that three types of electrocatalysts have been mainly investigated for this purpose: (i) enzymes, such as peroxidase [12]; (ii) noble metal catalysts, such as Pt, Au, Ag and Pd and their combinations [13-15]; and (iii) macrocycle complexes of transition metals, such as Co-porphyrin and Cu-triazine complexes [16, 17]. Enzymes exhibit biocompatibility and high activity for H_2O_2 electroreduction, but unfortunately, they frequently show relatively low chemical and thermal stability, which restricts their conditions of use. Noble metals are the most effective catalysts for H_2O_2 electrooxidation and electroreduction; however, they also catalyze the decomposition of H_2O_2 to O_2. Besides, they are relatively scarce and thus expensive, which hinder their use, particularly, for large-scale applications. Macrocycle complexes of transition metals suffer the drawback of inferior catalytic activity and instability in high concentrations of H_2O_2. Consequently, it is still of interest to develop alternate materials, in a cheap and effective way, for H_2O_2 electroreduction. Among the possible candidates to mitigate the mentioned drawbacks, transition metal oxides, such as copper, cobalt and ferric oxides, have captured considerable interest because of their variety of structures and properties, wide availability, low-cost and high electrochemical performances. In addition, the use of these oxides can prevent any surface oxidation of the electrode owing to their very good chemical stability, and it can also minimize the chemical decomposition of H_2O_2 on the electrode surface [18].

As part of our ongoing efforts to develop low-cost non-noble metal catalysts, we have already demonstrated in our previous work [19] the activity of copper films with granular structure and highlighted its competitiveness for the oxidation of formaldehyde in alkaline medium; herein, we report in the same way an easy electrochemical approach to prepare microstructured CuO films supported on Cu substrate for H_2O_2 electroreduction. Electrochemical experiments revealed that the obtained CuO/Cu electrodes exhibited excellent catalytic performance and good stability towards H_2O_2 electroreduction in alkaline medium.

In our study, however, we prepared our electrode material, using a simple deposition procedure, with the aim of using it as an alternative cathode catalyst to replace noble-metal catalysts commonly used in current fuel cells. And, we think that this study contributes a little to improving the use of fuel cells by using simple and available methods to develop active and less-expensive catalysts. We add that, in future activities and as part of our research in the field of fuel cells, this electrode material will be examined as a cathode catalyst in a fuel cell system with other less-expensive catalysts prepared by similar methods.

2. EXPERIMENTAL

2.1. Experimental details

CuO films were obtained from an aqueous solution of 5 M KOH (>99.0%) at room temperature (25 ± 0.5 C°) using a VoltaLab PGZ 301 potentiostat-galvanostat in three-electrode cell. A platinum wire and a saturated calomel electrode (SCE) were used as the counter and the reference electrode,

respectively. All potentials were referred to the SCE. Copper (Cu) foil (99.99% in purity) of 1 cm^2 area was assembled as the working electrode and was used as substrate for the preparation of our electrode.
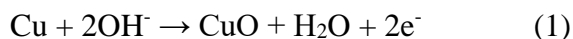
Before the electrochemical growth of CuO films, the Cu foil was first properly degreased in acetone for 5 min and then well rinsed with distilled water. Next, the cleaned Cu substrate was etched in a solution of 2 M hydrochloric acid (HCl) for 10 min and then rinsed several times with distilled water. This treatment aims to ensure strong adhesion and continuity of the oxide film. Afterward, the treated Cu foil was transferred to the electrochemical cell and used as working electrode to undergo the oxidation process. After the electrochemical reaction, the sample was finally removed from the solution, rinsed thoroughly with distilled water, and then allowed to air dry.

The surface morphology of the prepared electrodes was observed by a JEOL JCM-5000 scanning electron microscope. The crystallinity and crystal phase of the samples were examined using a Bruker D8 Advance X-ray diffractometer operating with high-intensity Cu (Kα) radiation source (λ = 1.5406 Å). The XRD patterns were obtained at 2θ = 30-100°. The electrocatalytic activity of the samples toward H_2O_2 reduction was investigated at room temperature using cyclic voltammetry and chronoamperometry techniques in 3 M KOH solution.

3. RESULTS AND DISCUSSION

3.1. Electrochemical preparation of CuO films

Figure 1 shows cyclic voltammogram recorded on Cu foil in 5 M KOH supporting electrolyte. The potential was swept between -375 to 0.0 mV in the anodic direction starting from the equilibrium potential of the electrode. The scan potential rate was 10 mV/s. At negative potentials of about -375 mV, no oxidation current was observed, suggesting that the electrode surface is free of oxide. However, as the electrode potential is scanned into the positive direction a sharp anodic peak around -215 mV (SCE) corresponds to the formation of CuO directly from Cu (Reaction 1) [20]. The beginning of the current increase was detected at -340 mV vs. SCE, which is characteristic of the over potential oxidation reaction of Cu electrode [21].
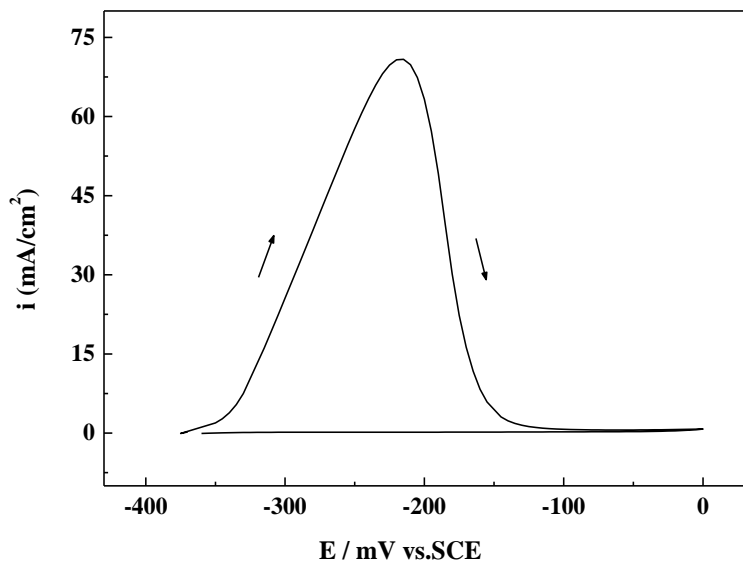
$$Cu + 2OH^- \rightarrow CuO + H_2O + 2e^- \qquad (1)$$

Figure 1. Cyclic voltammogram recorded on Cu foil electrode in 5 M KOH electrolyte solution. Scan rate = 10 mV/s.

3.2. Characterization of CuO/Cu

Figure 2 shows the XRD patterns at room temperature for the Cu foil before and after electrochemical oxidation. For both samples, the intense diffraction peaks appeared at 2θ values of 43.38°, 50.42°, 74.2°, 90° and 95.2° correspond respectively to the diffraction planes (111), (200), (220), (311) and (222) of the copper face-centered cubic (fcc) structure. [22].
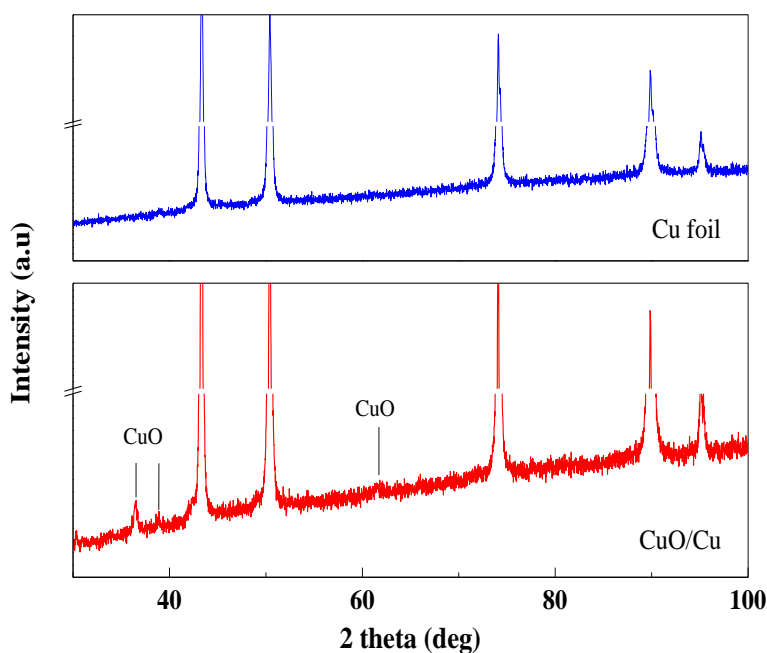

Figure 2. X-ray diffraction patterns for Cu foil and CuO/Cu. The surface morphology of the Cu foil before and after the formation of CuO is presented in
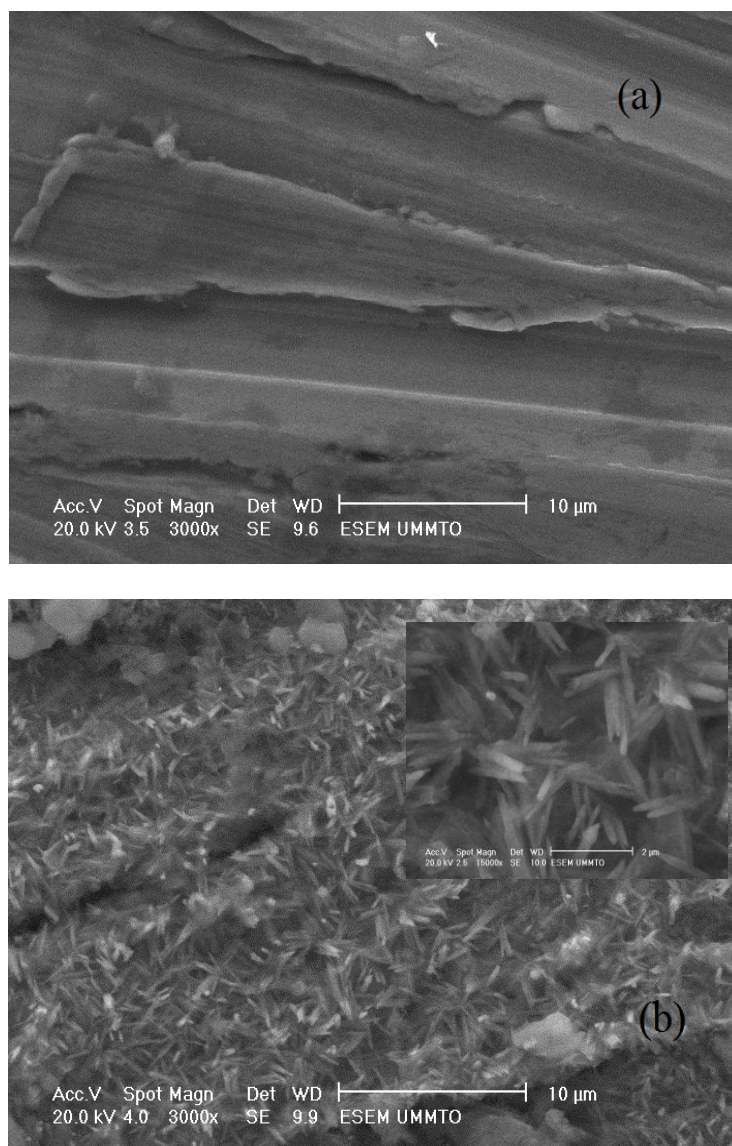
Figure 3. SEM micrographs of Cu foil surface: (a) before and (b) after growth of CuO film. Inset shows magnified image (×16000) of CuO film.
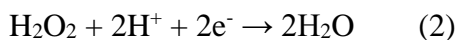
The XRD pattern of the oxidized Cu foil shows three additional diffraction peaks located at $2\theta = 36.4°$, $38.8°$ and $61.7°$ which can be indexed respectively to the (002)-(111), (200)-(111) and (113) planes of CuO monoclinic phase [20,23,24,25,26,27]. So, it can be concluded that the synthesized deposit is composed of CuO with monoclinic phase. The absence in the spectrum of other peaks related to other phases and impurities indicates the phase purity of CuO deposit. The broadening of CuO diffraction peaks is an indication of the presence of nanoscale crystallites. The mean crystallite size was found to be ~ 10 nm, using Scherrer's formula.

Figure 3 The SEM image of unmodified Cu foil has been recorded to compare its morphology and roughness with the surface of CuO/Cu electrode. Figure 3 (a) demonstrates the smooth texture of the unoxidized Cu foil. Figure 3 (b) clearly reveals that the oxidized sample gets completely covered by a homogenous and dense layer with a lawn-like microstructure. Interestingly, it can be seen from the

high-magnification view in the inset image in Figure 3 (b) that the formed CuO layer consists of an assembly of lots of needles (average length = 0.7-1 μm) of copper oxide that appear somehow randomly distributed over the entire surface of Cu foil. It is well established in literature that this type of growth of oxide enables the surface of the electrode to be highly accessible to the reactants and therefore increases the reactivity of the electrode for H_2O_2 electroreduction.

3.3. Electrocatalytic reduction of H_2O_2

Figure 4 shows cyclic voltammograms of CuO/Cu electrode recorded in 3 M KOH electrolyte in the absence and presence of different concentrations of H_2O_2. The electrode potential was swept at 10 mV/s scan rate in the potential range varying from -100 to -600 mV. In the absence of H_2O_2, it can be seen that no noticeable change in the current was observed over the entire potential range, indicating that no characteristic behavior was occurred on the electrode surface. In contrast, by adding H_2O_2 into the solution, a very important increase of the reduction current was recorded during the cathodic scan at potential value of -350 mV corresponding to the catalytic reduction of H_2O_2 which follows a two-proton and two-electron reaction (Eq. 2).

$$H_2O_2 + 2H^+ + 2e^- \rightarrow 2H_2O \qquad (2)$$

In figure 4, a wave appears at ~ -125 mV it due probably to oxygen dissolved. The H_2O_2 reduction peak is characterized by a large current density and low potentials, around – 0.3 V (SCE) which confirms that CuO layer, a good catalyst for the reduction of hydrogen peroxide when compared to different electrodes used for the reduction of H_2O_2 [20,28,29,30]. As can be seen that the cathodic currents are much larger in the presence of H_2O_2 than that without H_2O_2, and the currents increase with the increase of H_2O_2 concentration up to 0.4 M (Fig. 4). This demonstrated that electroreduction of H_2O_2 occurred on the CuO/Cu electrode. In addition, the cathodic current related to the hydrogen evolution reaction (HER) is observed at around -600 mV which is efficiently cathodic to enable the reduction of H_2O_2 without hydrogen evolution competition.

Figure 4 shows the cyclic voltammetric responses of the CuO/Cu electrode to various concentrations of H_2O_2 in 3 M KOH solution. As seen from this figure, the reduction peak current density increases gradually as the concentration of H_2O_2 increases. This indicates a typical electrocatalytic behavior of the CuO/Cu electrode towards the reduction of H_2O_2, and suggests that the use of high concentrations of H_2O_2 (of about 0.4 M) will boost the electrode performance when used as cathode for fuel cells using H_2O_2 as oxidant.
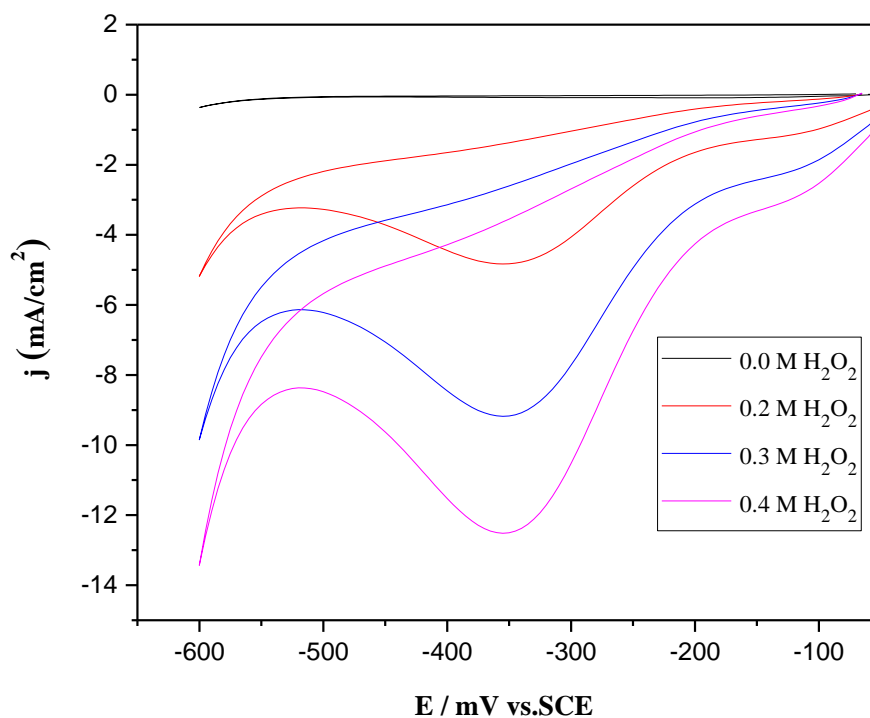
Figure 4. Cyclic voltammograms recorded on CuO/Cu electrode in 3 M KOH solution: in the absence and presence of three different concentrations of H_2O_2. Scan rate = 10 mV/s.

3.4. Stability of the CuO/Cu electrode

The stability of CuO/Cu electrode for H_2O_2 electroreduction was studied by chronoamperometry. Figure 5 shows chronoamperometric curves of H_2O_2 electroreduction on the CuO/Cu electrode at different constant potentials in 3 M KOH + 0.4 M H_2O_2 solution. The potentials were chosen in the active region from open-circuit potential (OCP) to the peak potential according to the cyclic voltammograms in Fig. 4. It can be clearly seen that by applying constant potentials to the electrode, the current densities associated with the electroreduction of H_2O_2 reached stationary state rapidly and showed no sign of decrease during the test period, which indicates that the CuO/Cu foil electrode possesses a good stability for catalyzing H_2O_2 electroreduction.
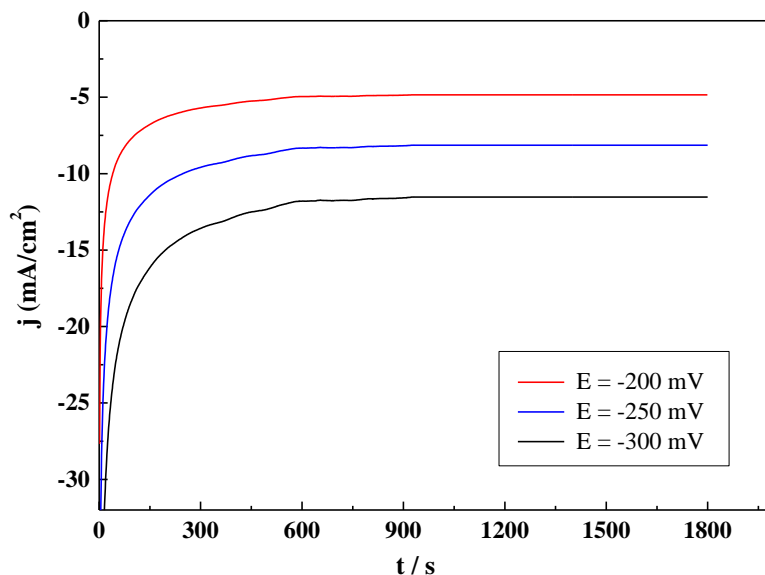
Figure 5. Chronoamperometric curves for H_2O_2 electroreduction on the CuO/Cu electrode at various constant potentials. Electrolyte: 3 M KOH + 0.4 M H_2O_2.

4. CONCLUSION

In this work, structured CuO film was successfully grown on Cu foil by a simple electrochemical procedure and investigated as a catalyst for H_2O_2 reduction in alkaline medium by cyclic voltammetry and chronoamperometry.

References

1.   D. Cao, Y. Gao, G. Wang, R. Miao, Y. Liu, *Int. J. Hydrogen Energy*, 35(2010)807.
2.   C.P. de León, F.C. Walsh, A. Rose, J.B. Lakeman, D.J. Browning, R.W. Reeve, *J. Power Sources*, 164(2007)441.
3.   A.K. Shukla, R.K. Raman, *Annu Rev Mater Res*., 33(2003)155.
4.   A.E. Sanli, A. Aytaç, *Int. J. Hydrogen Energy*, 36(2011)869.
5.   S. Yamazaki, Z. Siroma, H. Senoh, T. Ioroi, N. Fujiwara, K. Yasuda, *J. Power Sources*, 178(2008)20.
6.   D. Carriazo, J. Patino, M.C. Gutierrez, M.L. Ferrer, F. del Monte, *RSC Adv*., 3(2013)13690.

7.   A.V. Chadwick, S.L.P. Savin, S. Fiddy, R. Alcantara, D.F. Lisbona, P. Lavela, G.F. Ortiz, J.L. Tirado, *J. Phys.Chem*. C., 111(2007)4636.
8.   C. Yuan, J. Li, L. Hou, X. Zhang, L. Shen, X.W. Lou, *Adv. Funct. Mater*., 22(2012)4592.
9.   C. Yuan, L. Yang, L. Hou, L. Shen, X. Zhang, X.W. Lou, *Energy Environ. Sci*., 5(2012)7883.
10.   M.J. Aragon, B. Leon, C.P. Vicente, J.L. Tirado, A.V. Chadwick, A. Berko, S.Y. Beh, *Chem. Mater.*, 21(2009)1834.
11.   W. Jia, M. Guo, Z. Zheng, T. Yu, E.G. Rodriguez, Y. Wang, Y. Lei, *J. Electroanal. Chem*., 625(2009)27.
12.   W.N. Li, J. Yuan, X.F. Shen, S. Gomez-Mower, L.P. Xu, S. Sithambaram, M. Aindow, S.L. Suib, *Adv. Funct. Mater*., 16(2006)1247.
13.   L. Xu, Y.L. Hu, C. Pelligra, C.-H. Chen, L. Jin, H. Huang, S. Sithambaram, M. Aindow, R. Joesten, S.L. Suib, *Chem. Mater*., 21(2009)2875.
14.   S.M. Abdel Haleem, B.G. Ateya, *J. Electroanal. Chem*., 117(1981)309.
15.   G. Wang, J. Huang, S. Chen, Y. Gao, D. Cao, *J. Power Sources*, 196(2011)5756.
16.   T. Lei, Y. Tian, G. Wang, J. Yin, Y. Gao, Q. Wen, D. X. Cao, *Fuel Cell*, 11(2011)431.
17.   X. jing, D. Cao, Y. Liu, G. Wang, J. Yin, Q. Wen, Y. Gao, *J. Electroanal. Chem*., 658(2011)46.
18.   X. Guo, P. Diao, D. Xu, S. Huang, Y. Yang, T. Jin, Q. Wu, M. Xiang, M. Zhang, *Int. J. Hydrogen Energy*, 39(2014)7686.
19.   C. Dehchar, I. Chikouche, R. Kherrat, A. Sahari, A. Zouaoui, A. Merati, *Mater. Lett*., 228(2018)439.
20.   Y. Wan, X. Wang, H. Sun, Y. Li, K. Zhang, Y. Wu, *Int. J. Electrochem. Sci*.,7(2012)7902.
21.   Y. Li, D. Cao, Y. Liu, R. Liu, F. Yang, J. Yin, G. Wang, *Int. J. Hydrogen Energy*., 37(2012)13611.
22.   D.W. Lee, M.Y. Cho, I.S. Kim, Y.N. Kim, D. Lee, S.M. Koo, C. Park, J.M. Oh, *Surf Coat Tech*., 353(2018)66.
23.   F. Cao, T. Wang, X. Ji, *Appl. Surf. Sci*., 471(2019)417.
24.   S.R. Ardekani, A.S. Rouhaghdam, M. Nazari, *Chem. Phys. Lett*., 705(2018)19.
25.   V.X. Hien, N. H. Minh, D. T. Son, N. T. Nghi, L. H. Phuoc, C. T. Khoa, D. D. Vuong, N. D. Chien, Y.W. Heo, *Vacuum*, 150(2018)129.
26.   A.F. Zedan, N.K. Allam, S.Y. Aloaradawi, *Catalysts,* 7(2017)129.
27.   A. Hamam, D. Oukil, A. Dib, H. Hammache, L. Makhloufi, B. Saidani, *Surf Rev Lett*., 22(2015)1550065.
28.   D. Zhang, K.Ye, D. Cao, J.Yin, K. Cheng, B. Wang, Y. Xu, G. Wang, *J. Power Sources*, 273(2015)1142.
29.   G. Wang, Y. Bao, Y. Tian, J. Xia, D. Cao, *J. Power Sources*, 195(2010)6463.
30.   K. Cheng, F. Yang, Y. Xu, L. Cheng, Y. Bao, D. Cao, G. Wang, *J. Power Sources*, 240(2013)442.